



## Dispersive solid phase micro-extraction of mercury(II) from environmental water and vegetable samples with ionic liquid modified graphene oxide nanoparticles

ATEFEH NASROLLAHPOUR, SEYYED MOHAMMAD JAVAD MORADI  
and SEYYED ERSHAD MORADI\*

*Young Researchers and Elite Club, Islamic Azad University-Sari Branch, Sari, Iran*

(Received 13 October 2016, revised 10 March, accepted 13 March 2017)

**Abstract:** A new dispersive solid phase micro-extraction (dispersive-SPME) method for separation and preconcentration of mercury(II) using ionic liquid modified magnetic reduced graphene oxide (IL-MrGO) nanoparticles, prior to the measurement by cold vapour atomic absorption spectrometry (CV-AAS) has been developed. The IL-MrGO composite was characterized by Brunauer–Emmett–Teller method (BET) for adsorption-desorption measurement, thermogravimetric analysis (TGA), powder X-ray diffraction (XRD) and X-ray photo-electron spectroscopy (XPS). The method is based on the sorption of mercury(II) on IL-MrGO nanoparticles due to electrostatic interaction and complex formation of ionic liquid part of IL-MrGO with mercury(II). The effect of experimental parameters for preconcentration of mercury(II), such as solution type, concentration and volume of the eluent, pH, time of the sorption and desorption, amount of the sorbent and coexisting ion concentration have been optimized. Under the optimized conditions, a linear response was obtained in the concentration range of 0.08–10 ng mL<sup>-1</sup> with a determination coefficient of 0.9995. The limit of detection (*LOD*) of the method at a signal to noise ratio of 3 was 0.01 ng mL<sup>-1</sup>. Intra-day and inter-day precisions were obtained equal to 3.4 and 4.5 %, respectively. The dispersive solid phase micro-extraction of mercury(II) on IL-MrGO nanoparticles coupled with cold vapour atomic absorption spectrometry was successfully used for extraction and determination of mercury(II) in water and vegetable samples.

**Keywords:** mercury(II); ionic liquid; magnetic reduced graphene oxide; cold vapour atomic absorption spectrometry; dispersive solid phase micro-extraction.

\*Corresponding author. E-mail: er\_moradi@hotmail.com  
<https://doi.org/10.2298/JSC161013035N>

## INTRODUCTION

It has been included in the list of priority pollutants by the US EPA with a mandatory discharge limit of  $10 \mu\text{g L}^{-1}$  for wastewater and a maximum accepted concentration of  $1 \mu\text{g L}^{-1}$  in drinking water.<sup>1,2</sup> Considering the mercury contamination is widespread in the environment, the monitoring of mercury in the environment was imperative and critical for pollution prevention and control. The direct determination of mercury in water samples are atomic fluorescence spectrometry (AFS),<sup>3</sup> inductively coupled plasma mass spectrometry (ICP-MS),<sup>4</sup> inductively coupled plasma optical emission spectrometry (ICP-OES)<sup>5</sup> and cold vapour atomic absorption spectrometry (CV-AAS).<sup>6</sup> Although many analytical methods have been reported for the determination of mercury, most of them show limitations such as low sensitivity, susceptibility to interferences, time consuming and complicated or expensive instrumentation. Therefore, separation and preconcentration steps are often required to achieve accurate, sensitive and reliable results by an analytical method.

Several techniques including precipitation/co-precipitation,<sup>7</sup> liquid–liquid extraction,<sup>8</sup> cloud point extraction<sup>9</sup> and solid-phase extraction<sup>10</sup> (SPE) have been developed for the separation and the preconcentration of trace mercury(II). Among all methods, solid-phase extraction is the most common technique used for preconcentration of an analyte in environmental waters because of its advantages of high enrichment factor, high recovery, rapid phase separation, low cost, low consumption of organic solvents and the ability of combination with different detection techniques in the form of on-line or off-line mode.<sup>10,11</sup> In recent years a new kind of SPE, dispersive solid phase micro-extraction (dispersive-SPME), has attracted so much attention. The dispersive-SPME is based on the dispersion of the sorbent in the sample solution containing target analytes which allows complete interaction of the sorbent with analyte in a short period of time followed by a remarkable decrease in the required extraction time. Compared with other isolation methods, dispersive-SPME can improve the extraction efficiency and simplify the process of preprocessing.

The key point in sorbent-based extraction is the choice of proper sorbent, because it controls the analytical performance. Different sorbents including activated carbon,<sup>12</sup> zeolites,<sup>13</sup> carbon nanotubes,<sup>14</sup> modified magnetic particles,<sup>15</sup> modified silica,<sup>16</sup> magnetic molecularly imprinted microspheres<sup>17</sup> and graphene oxide<sup>18</sup> have been used in the dispersive-SPME procedure in recent years. Among these sorbents, graphene oxide due to its capabilities including ultrahigh surface area, good hydrophilicity and high dispersion stability<sup>19,20</sup> and unique physical and chemical properties has attracted great attention. GO possess large delocalized  $\pi$ -electron system and much polar oxygen functional groups, such as hydroxy, carboxy and epoxy groups, which enables GO interact with analytes through  $\pi-\pi$ , hydrogen bonding and electrostatic interactions. So, graphene

oxides have great potential as sorbents for the analysis of different compounds. However, according to our literature survey, the application of GO in real samples is limited due to its water instability and toxicity. So, it is highly needed to find a method to introduce some stable and specific functional moieties to GO. But the usage of graphene oxide as extracting phase is limited due to its high water solubility and consequently, the difficulty in its separation from the aqueous phase. The introduction of magnetic properties into graphene oxide can efficiently eliminate this limitation, because the sorbent is highly dispersed in the aqueous phase and no centrifugation is required for phase separation.

Ionic liquids (IL), is a kind of salt in which the ions are poorly coordinated. They have unique properties such as non-volatility, non-flammability, low viscosity, chemical and electrochemical stability, negligible vapor pressure and tunable miscibility. Thus, they are regarded as promising “green” materials for a number of analytical applications.<sup>21</sup> IL-modified materials have been successfully employed as extracting phases in solid phase extraction (SPE),<sup>22–24</sup> solid phase microextraction (SPME)<sup>25–27</sup> and dispersive solid phase microextraction (dispersive-SPME).<sup>28–31</sup>

Herein, the dispersive solid phase microextraction based on ionic liquid deposited on magnetic reduced graphene oxide (IL-MrGO) nanoparticles was developed for extracting mercury(II) in water and wastewater samples. The experimental parameters affecting on preconcentration of mercury(II) by dispersive-SPME method, such as solution pH, type, concentration and volume of the eluent, amount of the sorbent, time of the sorption and desorption, and coexisting ion concentration, were studied and optimized. The analysis of real sample and desorption experiment were further investigated. The proposed method has been applied for the determination of trace amounts of mercury(II) in water and vegetable samples.

## EXPERIMENTAL

### *Apparatus*

X-ray diffraction (XRD) measurements were carried out using a Rigaku D/max-rB diffractometer (Rigaku, Tokyo, Japan) with Cu-K $\alpha$  radiation (40 kV, 60 mA). The surface areas of samples were determined from nitrogen adsorption–desorption isotherms at liquid nitrogen temperature using a Coulter SA3100 instrument with outgas 15 min at 150 °C. The Brunauer–Emmett–Teller (BET) method was used for surface area calculation,<sup>32</sup> the pore size distribution (pore diameter, pore volume and micropore surface area of the samples) was determined by the Barrett–Joyner–Halenda (BJH) method.<sup>32</sup> X-ray photoelectron spectroscopy (XPS) was performed on Kratos Axis ULTRA X-ray photoelectron spectrometer equipped with monochromatic AlK $\alpha$  ( $h\nu = 1486.6$  eV) radiation to quantitatively analyzed the chemical composition of samples. Thermal analysis was carried out using Derivatograph Q-1500 D MOM (Hungary) equipment operated under a flow of an air at the heating rate of 10° min<sup>-1</sup>. A Varian SPECTRAA 20 plus (Palo Alto, CA, USA) cold vapour atomic absorption spectroscopy was used for determination of Hg(II) ions. Cold vapor of Hg was produced using a

vapor generation system (hydride generator, GBC HG 3000) and argon 99.99 % as the carrier, coupled to the atomic absorption spectrometer. Sodium borohydride was used as the reducing agent in the determination of mercury(II). The solution was freshly prepared containing 0.2 % NaBH<sub>4</sub> in 0.05 % NaOH. The other parameters are as follows: wavelength 253.7 nm, slit width 0.7 nm, lamp current 8 mA, argon flow 70 ml min<sup>-1</sup>, HCl concentration 3.0 mol L<sup>-1</sup> in water, reagent flow rate 1 mL min<sup>-1</sup> on each line, sample flow rate 7 mL min<sup>-1</sup>.

#### *Reagents and solutions*

The reactants of Graphite powder (<45 µm, ≥99.99 %), sodium peroxydisulfate (Na<sub>2</sub>S<sub>2</sub>O<sub>8</sub>, 99 wt.%), potassium permanganate (KMnO<sub>4</sub>, 99 wt.%), anhydrous ferric chloride (FeCl<sub>3</sub>, 99 wt.%), heptahydrate ferrous sulfate (FeSO<sub>4</sub>·7H<sub>2</sub>O, 99 wt.%) and phosphorus pentoxide (P<sub>2</sub>O<sub>10</sub>, 99 wt.%) were supplied by Merck Company (Darmstadt, Germany).

To synthesize the ionic liquid L-cysteine (99 %), 1-methylimidazole (99 %), catechol (CT, AR, 99%), *n*-Butyl bromide (99%), and hydroquinone (HQ, AR) were obtained from Sigma-Aldrich ((St. Louis, MO, USA). Hg(II) solution (1000 mg L<sup>-1</sup>) was prepared by dissolving appropriate amounts of HgCl<sub>2</sub> (99 wt.%, Merck, Germany) in distilled water. Working solutions were prepared by diluting the stock solution.

#### *Preparation of IL-MrGO*

For synthesis of IL-MrGO at first GO has been synthesized from method reported by our group.<sup>33</sup> In the second stage, MGO was prepared by co-precipitating Fe<sup>2+</sup> and Fe<sup>3+</sup> by sodium hydroxide solution in GO solution. Under the flow of argon, the ferric chloride (4 mmol) and ferrous sulfate (3.2 mmol) were dissolved in 50 mL GO (2 mg mL<sup>-1</sup>) solution. Chemical precipitation was achieved at 20 °C under vigorous stirring by adding sodium hydroxide solution (2.5 mol L<sup>-1</sup>). During the reaction process, the pH was maintained at about 10. After stirring for 1 h, the precipitates were washed several times with deionized water and finally dispersed in water with the concentration of 10 mg mL<sup>-1</sup>.

At final step, the ionic liquid loaded on magnetic reduced graphene oxide nanoparticles (IL-MrGO) was obtained according to a previous report of Wang and coworkers.<sup>34</sup> In a typical procedure, 0.5 g of the ionic liquid ([Bmim][Cys]) was put into 10 mL MGO aqueous suspension of 0.5 mg mL<sup>-1</sup>. The mixture was kept in a tightly sealed glass bottle and stirred for 15 h at room temperature. Firstly, the black product was isolated by centrifugation at 8000 rpm, and then the obtained black slurry was washed with deionized water. Then, one part of the as-prepared products was dispersed in deionized water to prepare the suspension of IL and MGO, and the other part was used to produce the powder of IL-MGO by drying at 50 °C for 24 h under vacuum. Finally, the mixture was refluxed for 12 h with continuous stirring. The product was filtered and washed with deionized water, and then dried at room temperature.

#### *Dispersive micro-solid phase extraction procedure*

At first, 2.0 mg of IL-MGO were transferred into a glass test tube containing 1.0 mL of deionized water and sonicated for 5 min. Then, the dispersed IL-MGO solution was injected rapidly to 20.0 mL sample solution (containing 2 µg L<sup>-1</sup> of Hg(II)) with a 1.0 mL syringe. At this stage, the analyte was absorbed into the dispersed sorbent. Subsequently, the IL-MGO was isolated from the solution by magnetic decantation and the upper phase was discarded. The supernatant was easily discarded, 100 µL of 0.10 mol L<sup>-1</sup> HNO<sub>3</sub> and 3 % thiourea was added to the residue and the mixture was sonicated for 4 min to desorb the retained mercury(II). Finally, the mixture was centrifuged at 5000 rpm for 2 min and the sorbent was held by the application of an external magnet and the mercury(II) in the eluent phase were deter-

mined by CV-AAS. The sorbent was regenerated through further washing with thiourea solution and rinsing with water for several times.

#### *Adsorption isotherms*

The amount of adsorbed Hg(II) was obtained using the following equation:

$$q_e = \frac{(c_0 - c_e)V}{m} \quad (1)$$

where  $q_e$  is the amount of Hg(II) adsorbed onto the unit amount of the IL-MrGO adsorbent ( $\text{mg g}^{-1}$ );  $c_0$  and  $c_e$  are the concentrations of Hg(II) in the medium before and after adsorption, respectively ( $\text{mg L}^{-1}$ );  $V$  is the volume of the adsorption medium (L);  $m$  is the amount of the IL-MrGO adsorbent (g).

#### *Real sample pretreatment for dispersive-SPME*

Water samples were collected from Tejen River, mineral water and sea water. The vegetable samples like potato, carrot and lettuce were purchased from supermarkets in Sari. Firstly, these samples were cleaned with double-distilled water and then dried at 85 °C. 5.0 g of celery and lettuce samples were transferred into separate PTFE digestion vessels. Afterwards, 10.0 mL of HNO<sub>3</sub> (65 %) and 5.0 mL of H<sub>2</sub>O<sub>2</sub> (30 %) were added and the vessels were heated on a hot plate at 80 °C for 36 h, till the clear transparent digests were obtained. The water samples were then stored in a refrigerator in the dark before analysis.

## RESULTS AND DISCUSSION

#### *Characterization*

The XRD patterns of Fe<sub>3</sub>O<sub>4</sub> NPs (Fe<sub>3</sub>O<sub>4</sub> nanoparticles), GO and IL-MrGO have been shown in Fig. S-1 of the Supplementary material. The Fe<sub>3</sub>O<sub>4</sub> NPs presents relative intensities of all diffraction peaks at  $2\theta$  30.251, 35.581, 43.211, 54.391, 57.091, 62.921 and 75.191°, that can be assigned to the reflections from (220), (311), (400), (422), (511), (440) and (533), respectively. The XRD pattern of IL-MrGO is similar to the experimental pattern for Fe<sub>3</sub>O<sub>4</sub> NPs and GO (the peak at  $2\theta$  29.421) with characteristic peaks at the same  $2\theta$  values which indicated the formation of graphene oxide and iron oxide nanoparticles in IL-MrGO structure. It indicating the right synthesis of IL-MrGO.

The nitrogen adsorption-desorption isotherms of graphene oxide and ionic liquid modified graphene oxide samples are shown in Fig. S-2 of the Supplementary material. In Table I, the specific surface area ( $S_{\text{BET}}$ ) and specific volume of the GO are 2302  $\text{m}^2 \text{ g}^{-1}$  and 0.88  $\text{cm}^3 \text{ g}^{-1}$ , respectively. The specific surface area and specific volume of IL-MrGO are reduced to 1454  $\text{m}^2 \text{ g}^{-1}$  and 0.62  $\text{cm}^3 \text{ g}^{-1}$ , respectively. Therefore, it may be assumed that ionic liquids or iron oxide nanoparticles are located inside the pores or near to the pore opening of reduced graphene oxide.

The composition of IL-MrGO was further characterized with TGA in a nitrogen environment at a heating rate of 10 °C min<sup>-1</sup> (Fig. S-3 of the Supplementary material). For IL-MrGO, MGO and GO, a slow weight loss at low temperature to 300 °C was observed, which could be assigned to the loss of the residual

solvent or remaining water. Then the other weight loss occurs from 300 to 600 °C, which might be assigned to the removal of ionic liquids and the release of CO and CO<sub>2</sub>. According to the weight changes of IL-MrGO, MGO and GO, about 46 and 32 wt. % of MGO and IL-MrGO is iron oxide nanoparticles, respectively. The difference in final weight percent of MGO and IL-MrGO clearly shows the loading of ionic liquid on MGO. Moreover, it shows a lower amount of oxygen containing groups in the IL-MrGO.

TABLE I. The surface area and porosity of GO and IL-MrGO samples

Sample	BET surface area, m <sup>2</sup> g <sup>-1</sup>	Pore volume, cm <sup>3</sup> g <sup>-1</sup>
GO	2302	0.88
IL-MrGO	1454	0.62

The chemical state of the iron of the Fe<sub>3</sub>O<sub>4</sub> NPs and IL-MrGO was examined by the XPS technique (Fig. S-4a of the Supplementary material). High resolution Fe 2p XPS spectrum of Fe<sub>3</sub>O<sub>4</sub> NPs shows that, the binding energy peaks at 711.1 and 724.6 eV in the high resolution Fe 2p scan correspond to Fe 2p<sub>3/2</sub> and Fe 2p<sub>1/2</sub>, respectively. High resolution Fe 2p XPS spectrum of IL-MrGO shows the peaks of Fe 2p<sub>1/2</sub> at about 723 and 727 eV, respectively, indicating the formation of mixed oxides of Fe (II) and Fe (III), such as Fe<sub>3</sub>O<sub>4</sub>.<sup>19</sup> It proves the right formation of Fe<sub>3</sub>O<sub>4</sub> phase in IL-MrGO sorbent. In order to explore the extent of reduction GO and the composition of IL-rGO, XPS analysis was conducted and the results are shown in Figure S-4b of the Supplementary material. In comparison to GO (29.6 %), IL-rGO has a weaker oxygen peak representing an atomic content of oxygen about 15.2 %.

#### Sorption capacity

In order to find the best sorbent, the capacity of the synthesized sorbents (Fe<sub>3</sub>O<sub>4</sub> NPs, GO, MGO and IL-MrGO) were calculated. To determine the adsorption capacity, 100 mg of sorbents were equilibrated with 100.0 mL of Hg(II) solutions (50-300 mg L<sup>-1</sup>) under optimum conditions (pH of 2.0, contact time of 5 h and agitation speed of 250 rpm). In order to evaluate the maximum adsorption capacity, the difference between concentration of the solution before and the concentration of the solution after extraction by the sorbent was calculated. The result has shown maximum adsorption capacity for mercury(II) (144.2 mg g<sup>-1</sup>) has been reached when the sorbent was IL-MrGO. Compared to Fe<sub>3</sub>O<sub>4</sub> NPs (15.3 mg g<sup>-1</sup>), GO (68.1 mg g<sup>-1</sup>) and MGO (100.9 mg g<sup>-1</sup>), IL-MrGO demonstrated better adsorption properties for mercury(II) because of its better interaction through a complex formation between L-cysteine in ionic liquid and Hg(II).<sup>2</sup>

### *Effect of pH on sorption*

The surface of the reduced graphene oxide has lower oxygen containing group in comparison to graphene oxide but it is a rich source of hydroxyl, epoxide and carboxyl groups. Moreover, L-cysteine in ionic liquid ([Bmim][Cys]) have functional groups of sulfur and amino acid. Accordingly, the pH of the sample solution has significant effect on the chemistry of IL-MrGO as well as the solution chemistry of metal ions. The zeta potentials of IL-MrGO nanoparticles at different pH were measured in the pH range 2.0–8.0. Figure 1 shows that the zeta potential values of the GO and IL-MrGO are negative and get more negative with the pH values. The negative surface charge of IL-MrGO provides the electrostatic attraction that is favorable for the adsorption of Hg(II) ions.

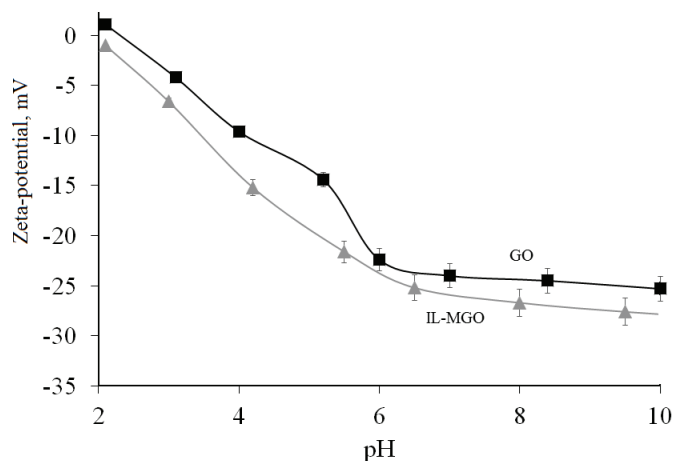


Fig 1. The pH effect on the Zeta potential of GO and IL-MrGO sorbent.

The effect of pH on the sorption of Hg(II) ( $2.0 \text{ ng mL}^{-1}$ ) is shown in Fig. 2. The pH of the analyte solution was adjusted by using hydrochloric acid (HCl) and sodium hydroxide (NaOH) in the pH range of 2.0 to 8.0. As can be seen from Fig. 2, the quantitative recovery was in the wide range of pH range (2.0–6.0). So, the recovery amounts of mercury(II) by the IL-MrGO was quantitative but best recovery value was at pH of 2.0. In this pH domain, mercury(II) is mainly cationic and IL-MrGO is anionic. So sorption is enhanced with the electrostatic interaction between the cations of Hg(II) and oxygen containing groups which located in the surface of IL-MrGO, and therefore, Hg(II) cations were reserved on the absorbent. Moreover, the L-cysteine in ionic liquid of IL-MrGO with Hg(II) can form mercury(II) dicysteinyl complex.<sup>2</sup> The formation of the complex can be explained by the theory of hard and soft acids and bases. Sulfur of L-cysteine is regarded as a soft donor atom that is inclined to combine with the soft metal like Hg(II).

*Effect of amount of IL-MrGO sorbent*

The effect of amounts of IL-MrGO on the sorption of 40.0 ng of Hg(II) from 20.0 mL of the sample solution was studied by varying the amount of the adsorbent within the range of 0.5–10.0 mg. The results (Fig. 3) showed that the recovery percent and satisfactory recoveries of Hg(II) to 2.0 mg of IL-MrGO and remained constant. Therefore, 2.0 mg of IL-MrGO was used in all subsequent experiments.

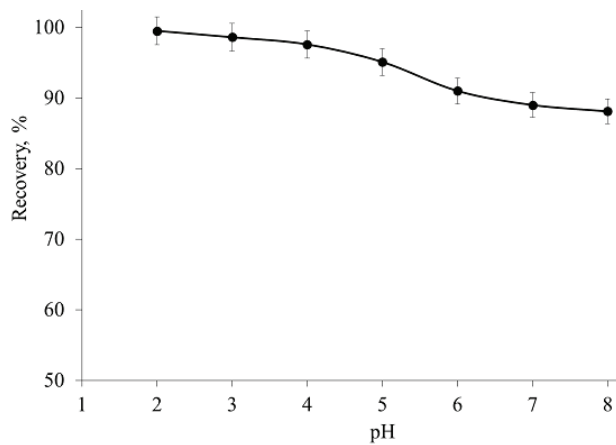


Fig. 2. Effect of solution pH on the recovery of Hg(II): IL-MrGO 2.0 mg; extraction time 60 s; desorption time 4 min; Hg(II) concentration 2  $\mu\text{g L}^{-1}$ ; solution volume 20.0 mL; eluent 0.10 mol  $\text{L}^{-1}$   $\text{HNO}_3$  and 3 % thiourea; eluent volume 100  $\mu\text{L}$ .

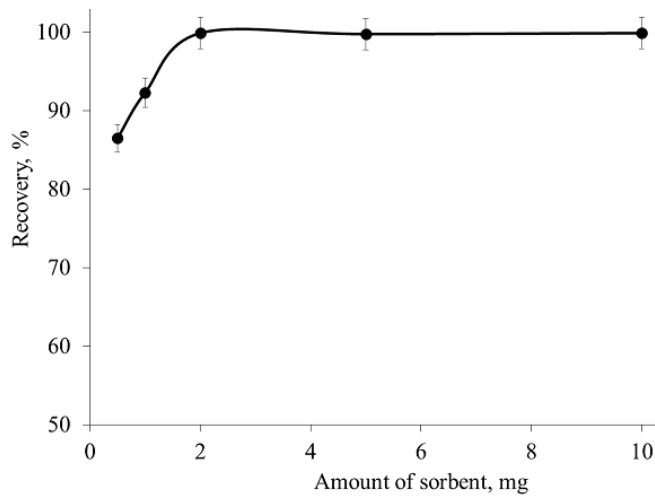


Fig. 3. Effect of sorbent amount on the recovery of Hg(II): pH 2.0; extraction time 60 s; desorption time 4 min; Hg(II) concentration 2  $\mu\text{g L}^{-1}$ ; solution volume 20.0 mL; eluent 0.10 mol  $\text{L}^{-1}$   $\text{HNO}_3$  and 3 % thiourea; eluent volume 100  $\mu\text{L}$ .

### *Effect of sorption and desorption time*

In solid phase extraction process, the sorption time is an important parameter which allows the appropriate dispersion of the sorbent throughout the sample solution and therefore generates a sufficient transfer time and contact area. To investigate the effect of extraction time on extraction efficiency of the Hg(II) by IL-MrGO, the contact time was varied from 0 to 5 min to investigate its effect on recovery of Hg(II). As shown in Fig. 4, after 60 s of equilibrium, the efficiency could increase to over 99 %. The rapid sorption equilibrium indicates the strong affinity between IL-MrGO and Hg(II). Also, investigations indicated that 4 min is adequate to desorb Hg(II) from sorbent surface.

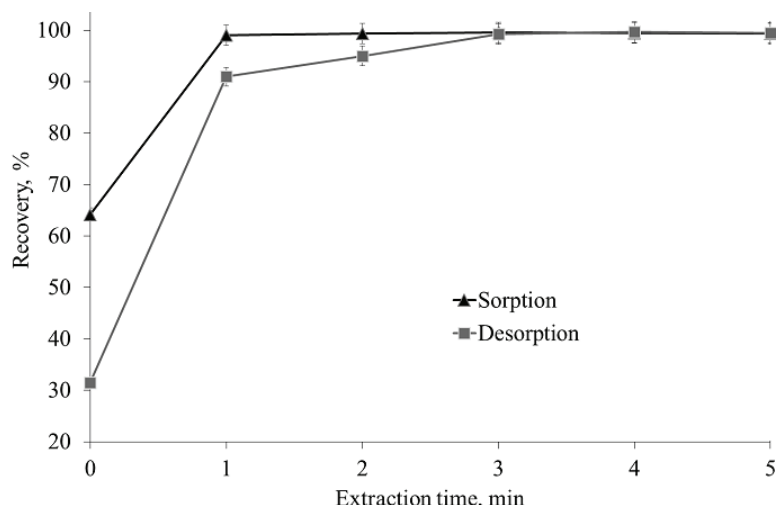


Fig. 4. Effect of sorption and desorption time on the recovery of Hg(II): IL-MrGO 2.0 mg; pH 2.0; Hg(II) concentration  $2 \mu\text{g L}^{-1}$ ; solution volume 20.0 mL; eluent  $0.10 \text{ mol L}^{-1}$   $\text{HNO}_3$  and 3 % thiourea; eluent volume 100  $\mu\text{L}$ .

### *Effect of the type and concentration of the desorption solvent on recovery*

To achieve more efficient desorption of analytes from sorbent surface and higher recovery, different eluents including acetic acid, nitric acid, hydrochloric acid or, nitric acid and thiourea were investigated in different concentrations. The results in Table II demonstrate that the highest recovery was obtained using  $0.1 \text{ mol L}^{-1}$  nitric acid and 3 % thiourea. Hence, it was chosen as desorption solvent system for further experiments.

In the next step, the effect of the volume of the desorbing solution on the extraction of mercury(II) was examined in the range of 50–250  $\mu\text{L}$ . According to the experiments, it was found that the maximum recovery of mercury(II) was obtained using 100  $\mu\text{L}$  of the desorption solvent.

### *Effect of sample volume*

As shown in Fig. 5, the recovery for the mercury(II) was obtained when the sample volumes were in the range of 5.0–40.0 mL. The results demonstrated that the recoveries of Hg(II) were quantitative up to 20.0 mL. The preconcentration factor can be calculated by ratio of the breakthrough volume and the eluent volume. As the Hg(II) in 20.0 mL of the sample solution were concentrated into 100 µL, an enrichment factor of 200 was determined by this method.

TABLE II. Effect of type and concentration eluent. IL-MrGO; 2.0 mg; pH 2.0; extraction time 60 s; desorption time 4 min; Hg(II) concentration 2 µg L<sup>-1</sup>; solution volume 20.0 mL; eluent volume 100 µL

Eluent	Concentration, mol L <sup>-1</sup>	Recovery, %
CH <sub>3</sub> COOH	0.05	85.6±2.2
CH <sub>3</sub> COOH	0.10	87.1±0.9
CH <sub>3</sub> COOH	0.20	89.2±1.5
HCl	0.05	88.4±1.0
HCl	0.10	89.1±2.4
HCl	0.20	90.8±1.9
HNO <sub>3</sub>	0.05	88.5±0.6
HNO <sub>3</sub>	0.10	91.6±1.0
HNO <sub>3</sub>	0.20	93.1±2.1
HNO <sub>3</sub> and thiourea	0.10 and 1%	96.5±0.7
HNO <sub>3</sub> and thiourea	0.10 and 3%	99.3±1.8
HNO <sub>3</sub> and thiourea	0.10 and 5%	99.4±1.1

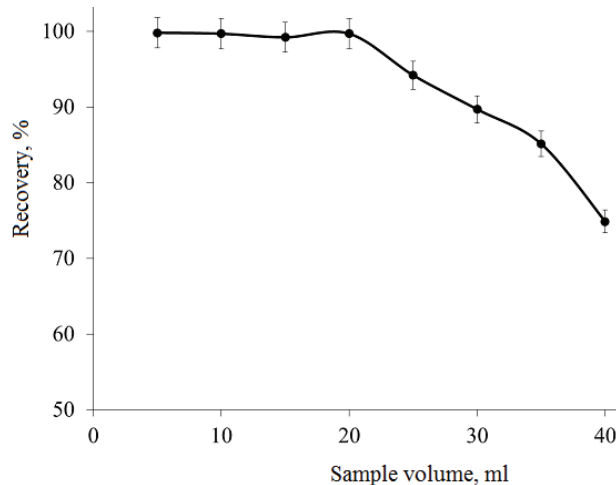


Fig. 5. Effect of sample volume on the recovery of Hg(II): IL-MrGO 2.0 mg; extraction time 60 s; desorption time 4 min; Hg(II) concentration 2 µg L<sup>-1</sup>; pH 2.0; eluent 0.10 mol L<sup>-1</sup> HNO<sub>3</sub> and 3 % thiourea; eluent volume 100 µL.

### *Effect of potentially interfering ions*

The interference of coexisting ions encountered in natural samples on the recovery of Hg(II) by proposed dispersive-MSPE method was investigated in the optimized conditions. The obtained results are given in Table III. Tolerable limit was defined as the highest amount of foreign ions that produced an error not exceeding  $\pm 5\%$  in the determination of the analyte ions. The recoveries of all analyte ions were quantitative for the given concentrations of interfering ions. The results demonstrate that coexisting ions have no significant effect on the analysis of Hg(II) from samples with a complex matrix.

TABLE III. Effects of coexisting ions on the determination of Hg(II). IL-MrGO 2.0 mg; pH 2.0; extraction time 60 s; desorption time 4 min; Hg(II) concentration 2  $\mu\text{g L}^{-1}$ ; solution volume 20.0 mL; eluent 0.10 mol  $\text{L}^{-1}$   $\text{HNO}_3$  and 3% thiourea; eluent volume 100  $\mu\text{L}$

Coexisting ion	Mole ratio, ion/Hg(II)	Recovery <sup>a</sup> , %
$\text{Na}^+$	10000	99.7 $\pm$ 1.8
$\text{K}^+$	10000	100.6 $\pm$ 0.4
$\text{Ca}^{2+}$	5000	98.4 $\pm$ 1.6
$\text{Zn}^{2+}$	150	99.9 $\pm$ 2.0
$\text{Ba}^{2+}$	150	99.6 $\pm$ 1.5
$\text{Mg}^{2+}$	5000	100.2 $\pm$ 1.3
$\text{Pb}^{2+}$	1000	99.5 $\pm$ 0.6
$\text{Cu}^{2+}$	1000	100.8 $\pm$ 1.5
$\text{Co}^{2+}$	150	99.8 $\pm$ 1.8
$\text{Fe}^{2+}$	900	101.9 $\pm$ 0.7
$\text{Mn}^{2+}$	700	99.8 $\pm$ 1.4
$\text{Fe}^{3+}$	100	99.1 $\pm$ 0.7
$\text{Cr}^{3+}$	100	99.1 $\pm$ 0.7
$\text{Al}^{3+}$	400	99.6 $\pm$ 1.9
$\text{Cl}^-$	10000	100.4 $\pm$ 1.4
$\text{NO}_3^-$	10000	100.7 $\pm$ 0.3
$\text{CO}_3^{2-}$	2000	99.8 $\pm$ 2.1
$\text{SO}_4^{2-}$	3000	99.4 $\pm$ 1.9

<sup>a</sup>Mean and standard deviation of three independent measurements

### *Analytical performance*

The analytical performance of dispersive-SPME-CV-AAS for the determination of Hg(II) was evaluated under the conditions already defined and the results are presented in Table IV. The standard curves after preconcentration by using the developed dispersive-SPME was linear in the range of 0.08–10  $\text{ng mL}^{-1}$  with calibration equation of  $A = 0.0201c + 0.0011$  and a good linearity ( $R^2 = 0.9995$ ). The standard curves and quantitative parameters including linear range, limits of detection ( $LOD$ ), limits of quantification ( $LOQ$ ), enrichment factor and relative standard deviations for this method were calculated under optimum conditions. The limits of detection ( $3S_b/b$ , where  $S_b$  is the standard deviation of blank and  $b$  is

the slope of calibration graph) and quantification ( $10S_b/b$ ) for Hg(II) extraction were found to be 0.01 and 0.04 ng mL<sup>-1</sup>, respectively. The relative standard deviations at 2 ng mL<sup>-1</sup> of mercury(II) ( $n = 6$ ) for the intra-day and the inter-day were 3.4 and 4.5 %, respectively. Considering the volumes of sample and eluent, the maximum preconcentration factor (PF) for this method was 200. They suggested that the developed method was of high sensitivity, wide linear range and good precision for Hg(II) determination.

A comparison of the analytical characteristic (including *LOD*, *RSD* and adsorption capacity, *PF*) obtained by this method with other reported dispersive-SPME methods<sup>35-40</sup> for the determination of Hg(II) is presented in Table IV. The obtained results indicated that in our method preconcentration factor was relatively high, the detection limit is low and precision is much better than other methods.

TABLE IV. Comparative data from some recent studies on solid-phase extraction of mercury

Sorbent	Analysis method	<i>RSD</i> / %	<i>LOD</i> / ng L <sup>-1</sup>	<i>PF</i>	Adsorption capacity, mg g <sup>-1</sup>	Ref.
Ion-imprinted polymethacrylic microbeads	CV-AAS	5	20	100	6.4	35
Graphene oxide-magnetic chitosan grafted with mercapto	CV-AAS	4.7	60	80	-	36
Dithizone functionalized Fe <sub>3</sub> O <sub>4</sub>	CV-AAS	11.1	50	250	111.4	37
EGBMA modified MSPT-MNPs <sup>a</sup>	CV-AAS	3.6	80	291	41.6	38
Chemically modified activated carbon with 1-acylthiosemicarbazide	ICP-OES	4	120	100	67.8	39
Nanometer silica functionalized by 2,6-pyridine dicarboxylic acid	ICP-AES	3.0	90	175	92	40
IL-MrGO	CV-AAS	3.4	10	200	144.2	This work

<sup>a</sup>Ethylene glycol bis-mercaptoacetate modified 3-(trimethoxysilyl)-1-propanethiol coated Fe<sub>3</sub>O<sub>4</sub> nanoparticles

#### *Accuracy and applicability of the method*

In order to confirm the applicability of the method, it was applied to the determination of mercury(II) in three real environmental water samples, *i.e.*, mineral water, river water and sea water samples beside two vegetable samples. The suitability of the developed method was checked by spiking samples with a known amount of mercury(II) before sample digestion. The results given in the Table V, shows that the percent recoveries in the range of 97.8–100.8 %. The

obtained recoveries show that a good agreement was obtained between the certified results and found analyte contents. On the other hand, based on the results of Table V, it could be concluded that despite the 200 fold-times preconcentration factor, it was still not enough to determine Hg in the evaluated real samples.

TABLE V. Results for the determination of Hg(II) in real samples ( $n = 3$ ). IL-MrGO 2.0 mg; pH 2.0; extraction time 60 s; desorption time 4 min; Hg(II) concentration 2  $\mu\text{g L}^{-1}$ ; solution volume 20.0 mL; eluent 0.10 mol  $\text{L}^{-1}$   $\text{HNO}_3$  and 3 % thiourea; eluent volume 100  $\mu\text{L}$

Sample	Added	Found <sup>a</sup>	Recovery, %
River water, $\mu\text{g L}^{-1}$	0	N.D. <sup>b</sup>	—
	2	1.97±0.04	98.5
	10	10.08±0.32	100.8
mineral water, $\mu\text{g L}^{-1}$	0	N.D.	—
	2	1.99±0.05	99.5
	10	9.96±0.24	99.6
Sea water, $\mu\text{g L}^{-1}$	0	N.D.	—
	2	2.08±0.04	100.4
	10	9.86±0.19	98.6
Celery, $\mu\text{g g}^{-1}$	0	N.D.	—
	2	1.98±0.03	99.0
	10	11.41±0.33	97.8
Lettuce, $\mu\text{g g}^{-1}$	0	N.D.	—
	2	2.01±0.05	102.0
	10	9.97±0.17	99.7

<sup>a</sup>Mean and standard deviation of three independent measurements; <sup>b</sup>not detected

## CONCLUSION

In this study, dispersive-SPME technique was successfully applied for separation, determination, and preconcentration of mercury(II) in environmental and vegetable samples. Due to the presence of the iron oxide NPs and ionic liquid and ordered structure of IL-MrGO possesses high adsorption capacity, fast sorption and elution kinetics for mercury(II) and easily magnetic separation from the sample solution. Compared with the other established methods, the developed method provided high enrichment factor, low LODs, wide linear range, high throughput and selectivity.

## SUPPLEMENTARY MATERIAL

XRD patterns,  $\text{N}_2$  sorption isotherms, TGA curves and XPS spectra of the investigated compounds are available at the pages of journal website: <http://www.shd.org.rs/JSCS/>, or from the corresponding author on request.

## ИЗВОД

ДИСПЕРЗИВНА ЕКСТРАКЦИЈА ЧВРСТОМ ФАЗОМ ЖИВЕ(II) ИЗ ВОДА ОКОЛИНЕ И  
БИЉНИХ УЗОРАКА ПОМОЋУ НАНОЧЕСТИЦА РЕДУКОВАНОГ ОКСИДА ГРАФЕНА  
МОДИФИКОВНИХ ЈОНСКОМ ТЕЧНОШЋУ

ATEFEH NASROLLAHPOUR, SEYYED MOHAMMAD JAVAD MORADI и SEYYED ERSHAD MORADI

*Young Researchers and Elite Club, Islamic Azad University-Sari Branch, Sari, Iran*

Развијена је нова дисперзивна микро-екстракција чврстом фазом за сепарацију и преконцентрисање живе(II) уз коришћење наночестица редукованог оксида графена модификованог јонском течношћу (IL-MrGO), пре мерења атомском апсорпционом спектрометријом хладних пара (CV-AAS). У карактеризацији композита IL-MrGO примењене су Brunauer–Emmett–Teller метода (BET), термогравиметријска анализа (TGA), дифракција X-зрака (XRD) и фотоелектронска спектроскопија X-зрака (XPS). Метода је базирана на сорпцији живе(II) на наночестицама IL-MrGO захваљујући електростатичким интеракцијама и формирању комплекса са јонском честицом течношћу композита и живе(II). Оптимизовани су услови за преконцентрацију живе(II), као што су тип раствора, концентрација и запремина елуента, pH, време сорпције и десорпције, количина сорбента и концентрација коегзистирајућих јона. Под оптималним условима линеарни линеарна зависност одговора је добијена у концентрационом опсегу  $0,08\text{--}10 \text{ ng mL}^{-1}$  са коефицијентом од 0,9995. Лимит детекције методе (*LOD*) у односу на однос сигнал/шум од 3/1 износи  $0,01 \text{ ng mL}^{-1}$ . Прецизност резултата у једном дану, односно више дана, износи 3,4 и 4,5 %, редом. Дисперзивна микро-екстракција чврстом фазом живе (II) на наночестицама IL-MrGO у комбинацији са атомском апсорпционом спектрометријом хладних пара је успешно примењена за екстракцију и одређивање живе(II) у узорцима вода и поврћа.

(Примљено 13. октобра 2016, ревидирано 10. марта, прихваћено 13. марта 2017)

## REFERENCES

1. F. E. Chigbo, R. W. Smith, F. L. Shore, *Environ. Pollut., A* **27** (1982) 31
2. R. K. Zalups, *Pharmacol. Rev.* **52** (2000) 113
3. D. Sanchez-Rodas, W. T. Corns, B. Chen, P. B. Stockwell, *J. Anal. At. Spectrom.* **25** (2010) 933
4. M. Bettinelli, S. Spezia, A. Ronchi, C. Minoia, *Rapid Commun. Mass Spectrom.* **16** (2002) 1432
5. B. B. A. Francisco, A. A. Rocha, P. Grinberg, R. E. Sturgeon, R. J. Cassella, *J. Anal. At. Spectrom.* **31** (2016) 751
6. D.-Q. Zhang, L.-L. Yang, H.-W. Sun, *Anal. Chim. Acta* **395** (1999) 173
7. W. Jiang, J. Lv, L. Luo, K. Yang, Y. Lin, F. Hu, J. Zhang, S. Zhang, *J. Hazard. Mater.* **262** (2013) 55
8. R. A. Vanderpool, W. T. Buckley, *Anal. Chem.* **71** (1999) 652
9. T. d. A. Maranhão, E. Martendal, D. L. G. Borges, E. Carasek, B. Welz, A. J. Curtius, *Spectrochim. Acta, B* **62** (2007) 1019
10. Y. Liu, X. Chang, S. Wang, Y. Guo, B. Din, S. Meng, *Anal. Chim. Acta* **519** (2004) 173
11. L. Berthod, G. Roberts, D. C. Whitley, A. Sharpe, G. A. Mills, *Water Res.* **67** (2014) 292
12. S. Cerutti, M. F. Silva, J. A. Gásquez, R. A. Olsina, L. D. Martinez, *Spectrochim. Acta, B* **58** (2003) 43

13. S. L. C. Ferreira, J. B. de Andrade, M. d. G. A. Korn, M. d. G. Pereira, V. A. Lemos, W. N. L. d. Santos, F. d. M. Rodrigues, A. S. Souza, H. S. Ferreira, E. G. P. da Silva, *J. Hazard. Mater.* **145** (2007) 358
14. G. Lasarte-Aragonés, R. Lucena, S. Cárdenas, M. Valcárcel, *Anal. Bioanal. Chem.* **405** (2013) 3269
15. J. Qiao, M. Wang, H. Yan, G. Yang, *J. Agric. Food. Chem.* **62** (2014) 2782
16. F.-J. Liu, C.-T. Liu, W. Li, A.-N. Tang, *Talanta* **132** (2015) 366
17. C. Chen, X. Zhang, Z. Long, J. Zhang, C. Zheng, *Microchim. Acta* **178** (2012) 293
18. M. Ghorbani, M. Chamsaz, G. H. Rounaghi, *J. Sep. Sci.* **39** (2016) 1082
19. V. Chandra, J. Park, Y. Chun, J. W. Lee, I.-C. Hwang, K. S. Kim, *ACS Nano* **4** (2010) 3979
20. J. Sun, Q. Liang, Q. Han, X. Zhang, M. Ding, *Talanta* **132** (2015) 557
21. B. Zawisza, R. Sitko, E. Malicka, E. Talik, *Anal. Methods* **5** (2013) 6425
22. H. Yan, M. Gao, J. Qiao, *J. Agric. Food. Chem.* **60** (2012) 6907
23. P. Su, R. Wang, Y. Yu, Y. Yang, *Anal. Methods* **6** (2014) 704
24. L. Vidal, M.-L. Riekkola, A. Canals, *Anal. Chim. Acta* **715** (2012) 19
25. F. O. Pelit, L. Pelit, T. N. Dizdaş, C. Aftafa, H. Ertaş, E. E. Yalçınkaya, H. Türkmen, F. N. Ertaş, *Anal. Chim. Acta* **859** (2015) 37
26. M. Cordero-Vaca, M. J. Trujillo-Rodríguez, C. Zhang, V. Pino, J. L. Anderson, A. M. Afonso, *Anal. Bioanal. Chem.* **407** (2015) 4615
27. T.-T. Wang, Y.-H. Chen, J.-F. Ma, M.-J. Hu, Y. Li, J.-H. Fang, H.-Q. Gao, *Anal. Bioanal. Chem.* **406** (2014) 4955
28. F. Galán-Cano, R. Lucena, S. Cárdenas, M. Valcárcel, *Microchem. J.* **106** (2013) 311
29. D. Han, B. Tang, K. H. Row, *Anal. Lett.* **46** (2013) 2359
30. H. Yan, M. Gao, C. Yang, M. Qiu, *Anal. Bioanal. Chem.* **406** (2014) 2669
31. N. Fasih Ramandi, F. Shemirani, *Talanta* **131** (2015) 404
32. G. Fagerlund, *Mater. Constr.* **6** (1973) 239
33. S. E. Moradi, *Appl. Phys., A* **119** (2015) 179
34. C. Wang, Y. Chen, K. Zhuo, J. Wang, *Chem. Commun.* **49** (2013) 3336
35. I. Dakova, I. Karadjova, V. Georgieva, G. Georgiev, *Talanta* **78** (2009) 523
36. E. Ziaeи, A. Mehdinia, A. Jabbari, *Anal. Chim. Acta* **850** (2014) 49
37. L. Adlnasab, H. Ebrahimzadeh, A. A. Asgharinezhad, M. N. Aghdam, A. Dehghani, S. Esmaeilpour, *Food. Anal. Method.* **7** (2014) 616
38. M. H. Mashhadizadeh, M. Amoli-Diva, M. R. Shapouri, H. Afruzi, *Food Chem.* **151** (2014) 300
39. R. Gao, Z. Hu, X. Chang, Q. He, L. Zhang, Z. Tu, J. Shi, *J. Hazard. Mater.* **172** (2009) 324
40. L. Zhang, X. Chang, Z. Hu, L. Zhang, J. Shi, R. Gao, *Microchim. Acta* **168** (2010) 79.